Liquid-Gas Distribution Measurements in the Pulsing Regime of Two-Phase Concurrent Flow in Packed Beds

W. E. BEIMESCH and D. P. KESSLER

School of Chemical Engineering
Purdue University, Lafayette, Indiana 47907

The most extensive operating flow rate range in liquid-gas downward concurrent flow in a packed bed is the pulsing regime. In this flow regime liquid and gas traverse the bed in the form of segregated slugs, as shown in Figure 1. Since in many chemical reactions, the rate of mass transfer to and from the catalyst surface and radial heat transfer are extremely important, we have studied the phase distribution within these segregated slugs.

Large throughputs are one of the prime reasons for using concurrent two-phase systems for a reactor, which is typified by hydrodesulfurization, hydrocracking, liquid phase oxidation and hydrogenation reactions in the petroleum industry.

In the past ten years, work has been done regarding flow regime boundaries, pressure drop, liquid holdup, and pulse characteristics (*2, 5, 6, 9, 12, 14, 15*). Figure 2 shows the boundaries of the different flow regimes as found by Weekman (*14*) and verified by Wulfert (*15*) for the packings used in this study. Weekman (*13*) and Reiss (*9*) have studied the radial liquid-gas distribution in a concurrent system. Reiss concluded that radial liquid distribution was a function of packed-bed height, and gas and liquid rates expressed in the two-phase parameter χ. The flow regime of operation was not mentioned. Weekman found that the liquid flow tended to concentrate near the wall and also at the center of the bed. Increasing the air rate had the general effect of giving a more uniform radial liquid distribution. Hoftyzer (*4*) and Prost (*8*) employed an electrical conductance technique to study liquid distribution on the packing in the gas continuous regime. Using dumped Raschig rings, Hoftyzer found an irregular distribution of liquid in which the greater part of the liquid flowed over 5% of the surface, and 50% of the surface was hardly wetted. Prost concluded that the velocity and direction of gas flow influenced the local characteristics of the liquid. Hoffman and Effron (*3*) used a tracer technique to measure residence time distributions for liquid and gas phases. They proved that in a gas continuous regime there were little radial liquid or gas velocity gradients.

The objectives of this research were to determine quantitatively the distribution of one phase in the other in the pulsing flow regime and to determine the effects of the variables involved.

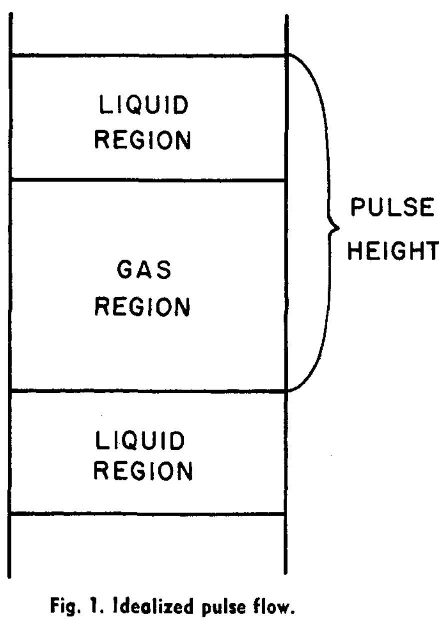

Fig. 1. Idealized pulse flow.

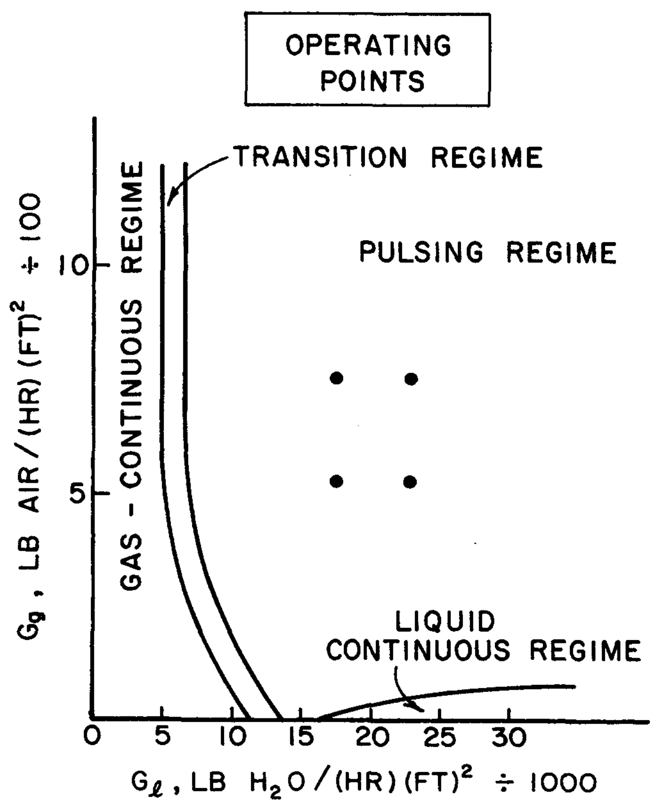

Fig. 2. Observed flow regimes by Wulfert.

Correspondence concerning this article should be addressed to Professor D. P. Kessler.

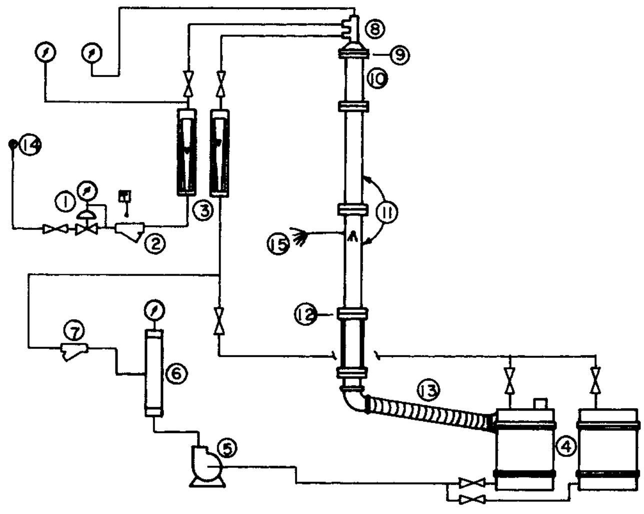

Fig. 3. Experimental apparatus.

An electrical conductance probe was used to determine the presence of liquid or gas at a point in the bed. The variables studied in this work were liquid rate, gas rate, packing size, and radial position in the packed bed.

EXPERIMENTAL SECTION

Equipment

The equipment used for the experimental work is shown in Figure 3. Weekman (*14*) and Wulfert (*15*) employed the same equipment in their studies.

Rotameters were available to meter the flows of air and water. Pressure gauges measured outlet rotameter pressure and column top pressure.

A centrifugal pump moved the water through a damping chamber, strainer, and rotameter. The damping chamber was a 3-in. standpipe with air trapped at the top. This piece of equipment minimized fluid fluctuations. A 20-mesh screen strainer removed particulate matter in the water.

The air passed through a strainer, pressure regulator, and rotameter. The strainer contained a 40-mesh screen packed tightly with steel wool; this prevented any oil or particulate matter from passing to the column. A pressure regulator and rotameter controlled the flow of air and maintained the operating pressure at 8 lb./sq. in. gauge at the head of the column. All runs were made at this pressure.

Figure 3 shows the three main sections of the experimental column; column head, top, and test. The column head provided the entrance for both air and water. The packed top section was 10 in. long and served to eliminate entrance effects (*14*). The beginning of the top section consisted of a ¼-in. thick aluminum distribution plate with 97 evenly spaced 11/64-in. holes. The top section was always packed to within ½-in. of the distribution plate.

Two 2-ft. pieces of Bakelite pipe flanged together contained the packed test section. The bottom piece also served as the support for the probes used in this study. Six and one-half in. down on the outside wall of the second bottom section, four pipe taps were drilled in the same horizontal plane. These holes were 90 deg. apart on the circumference of the pipe.

A mesh, made from 1/64-in. galvanized wire with ⅛-in. squares, supported the packing.

Electrical System and Probes

The probes were made from 22 AWG tin-copper Belden hookup wire and supported in copper tubing. The plastic-covered wire was coated with a layer of epoxy resin to give it strength. Figure 4 shows the probe used to measure the volumetric liquid fraction at a point. A power supply maintained an 8-v. potential across the probe gap. When water bridged the gap, the circuit was closed, allowing current to flow. When air passed, the circuit opened and no current flowed. By proper arrangement four probes could be used at one time to verify angular symmetry in the bed.

A layer of enamel provided a hydrophobic surface and enabled the probe to shed water immediately. Probe style No. 2 had an additional piece of wire on the top and bottom to prevent packing from lodging in the probe opening and inhibiting sufficient water shedding. Both probe styles were such that it was impossible for the packing to come into contact with the wire tips and cause interference.

The resistance of the probes with gaps shorted by water measured about 25,000 ohms. A four-channel strip chart recorder traced the electrical voltage across the resistor shown in Figure 4. No signal attenuation occurred in the recorder up to 3,000 cycles/sec., which was much higher than the disturbance frequency at the probe tips.

Calibration of the Probe

Before using the probe to obtain quantitative information, it was necessary to calibrate its response as a function of the volumetric gas fraction in the liquid. In a system similar to that shown in Figure 5, Nicklin (*7*) performed a series of experiments to determine the volumetric gas fraction of a bubbly system. Wallis (*10*) represented a bubbly system where gas is bubbled through a stagnant liquid by the empirical equation

$$V_{SG} = V_{\infty}(\alpha_T)(1 - \alpha_T)^{n-1} \quad (1)$$

In the calibration system of Figure 5, the bubble diameter was regulated by the air rate through the porous fritted glass to make $n = 1$ and $V_{SG} = V_{\infty}(\alpha_T)$ in Equation (1). The probe was centered in the calibration tube; its response was recorded as a function of the gas flow rate. The areas under the trace curves were integrated and compared to the total area (between the liquid continuous and gas continuous base lines) as shown in an idealized response in Figure 6. The data obtained were estimated time-averaged values of the volumetric liquid fraction at the probe over the operating sample time. Eight to nine sec. running time of calibration traces was integrated for each data point.

Several direct measurements of volumetric air fraction were taken by the difference in the liquid levels to verify the expression $V_{SG} = V_{\infty}(\alpha_T)$ for this system. As seen in Figure 5, the liquid level in the tube exceeds the liquid level in the reservoir drum. The difference in this liquid height divided by the total liquid height in the calibration tube gave the volumetric gas fraction present in the tube.

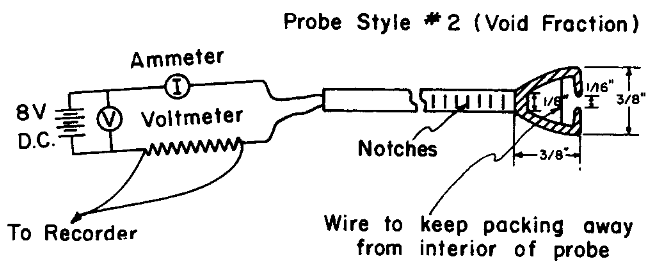

Fig. 4. Probe and circuit.

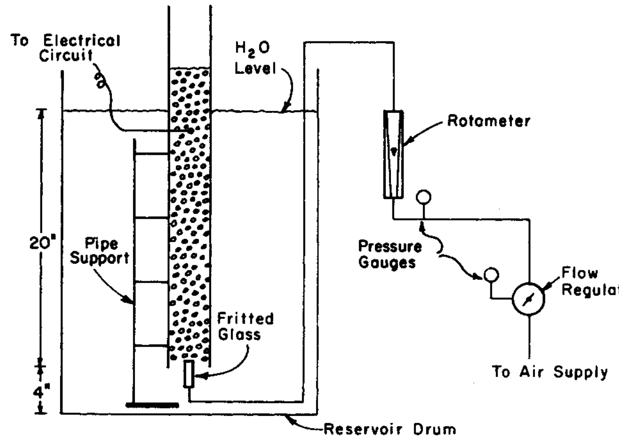

Fig. 5. Probe calibration system.

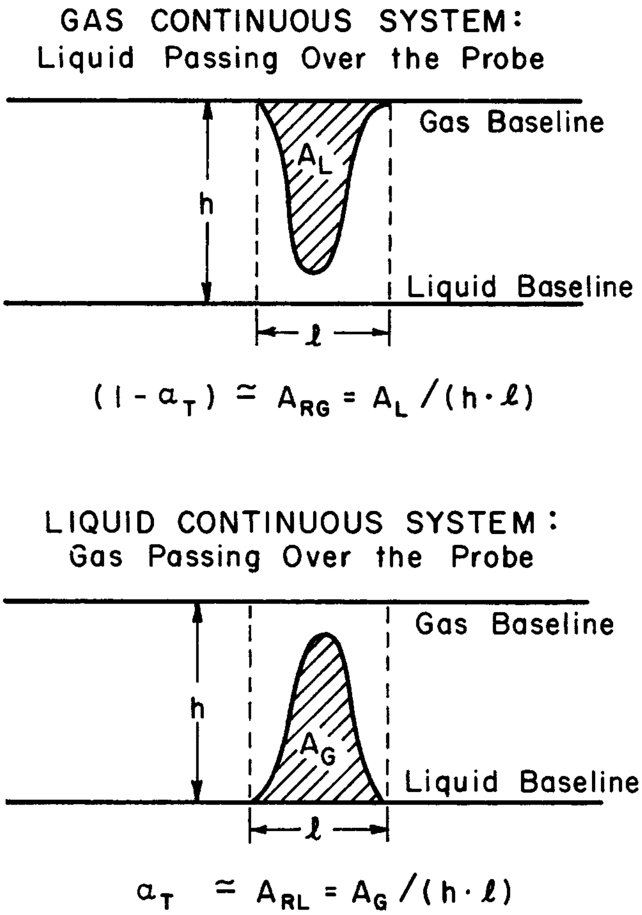

Fig. 6. Analogy of probe in liquid and gas continuous media.

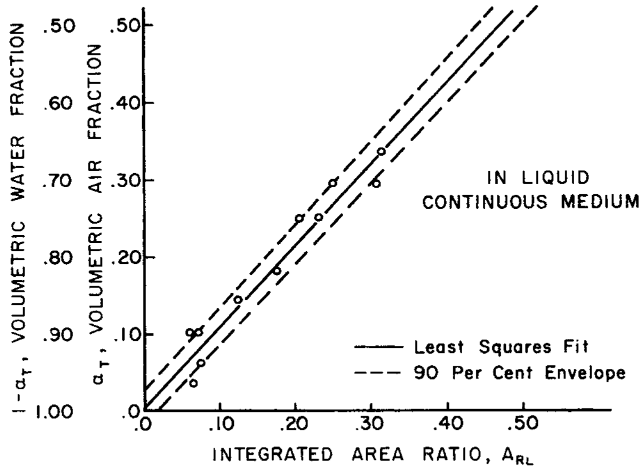

Fig. 7. Probe calibration curve.

Figure 7 shows a plot of volumetric air fraction versus integrated area ratio with 90% confidence limits on the line. A least squares fit gives

$$\alpha_T = 0.007 + 1.040\ A_{RL}$$

or

$$\alpha_T \simeq A_{RL}$$

or

$$(1 - \alpha_T) \simeq A_{RG}$$

Therefore the probe was assumed to be volumetrically sensitive. In a gas continuous system of 10% by liquid volume, the probe will give the same integrated area ratio as a liquid continuous system of 10% gas, that is, the probe response is the same.

Experimental Procedure

The column was run under pulse flow conditions for at least 10 min. before data were taken to ensure thorough wetting of the bed.

The variables were arranged in a 2 × 2 × 2 × 6 factorially designed experiment as follows:

Liquid rates	17,500 and 22,500 $lb._m/(hr.)(sq.ft.)$
Gas rates	525 and 750 $lb._m/(hr.)(sq.ft.)$
Packing	
glass beads;	$\epsilon = 0.387$; $D_p = 0.185$ in.
alumina spheres;	$\epsilon = 0.444$; $D_p = 0.254$ in.

Positions of probe in the packed 3-in. column

$r/r_0 = 0, 1/6, 1/3, 1/2, 2/3, 5/6$

Once the trace for given gas and liquid flow rates was obtained, the regulators were adjusted to the next level of flow. The flow rates were allowed to steady out before data were taken. For each probe position, data were taken for water and air settings in a 2 × 2 factorial design. The column was unpacked and repacked for each change in the probe position.

From the traces, five randomly selected pulses were chosen. The areas under the curves were integrated by counting 1 mm. squares on the paper. Reproducibility in counting the squares averaged 4%.

TABLE 1. ANALYSIS OF VARIANCE

L data compared with *H* data

Source of variation	Degrees of freedom	Sums of squares	Mean squares	*F* value	Result
Packing	1	0.12331	0.12331	119	+
Liquid rate	1	0.00151	0.00151	1.42	Not sign.
Gas rate	1	0.11607	0.11607	110	+
Position in the bed	5	2.32438	0.46488	437	+
Packing/liquid rate interaction	1	0.00000	0.00000	0.000	Not sign.
Packing/gas rate interaction	1	0.00626	0.00626	5.92	*
Packing/probe position in the bed interaction	5	0.21889	0.04378	41.2	+
Liquid rate/gas rate interaction	1	0.00060	0.00060	0.558	Not sign.
Liquid rate/position in the bed interaction	5	0.00609	0.00122	1.15	Not sign.
Gas rate/position in the bed interaction	5	0.00796	0.00159	1.50	Not sign.
Due to error	213	0.22644	0.00106		
Total	239	3.03151			

+ Highly significant; $P \leq 1\%$. * Significant; $1\% \leq P \leq 5\%$. ± Possibly significant; $5\% < P \leq 10\%$.
Sum of squares due to error is the sum of variation within replicates plus all third- and fourth-order interactions.
The *F* value is determined by comparing the mean square of the effect to the mean square due to error.

RESULTS AND DISCUSSION

The analysis of variance (Table 1) shows the results of the factorial design.

Packing Effect

The main effect due to the packing was statistically significant. Experimentally, the resistance to flow through a bed of smaller porosity has been shown to be greater than for the same flow through a bed of higher ranges of porosity. The higher resistance to flow in the smaller diameter spheres treated here indicates that the smaller diameter spheres support proportionately more liquid than the larger spheres under the same liquid and gas flow conditions. Figure 8 shows that the primarily liquid portion of the pulse is more dense in the lower porosity packing under the same flow conditions.

Liquid Rate Effect

The main effect due to the liquid flow rate was not significant. As liquid flow rate increases, the total liquid holdup in the column increases. However, this increased total liquid holdup appears in the increased height of the primarily liquid portion of the pulse. According to Weekman's work (*14*), at a constant gas flow rate, there is not a large increase in the velocity of the pulse when the liquid flow rate is varied in this region. The essential fluid mechanics do not change, the liquid portion just gets longer (at constant gas flow rates).

Gas Rate Effect

The main effect due to the gas flow rate was significant. At a constant liquid flow rate, increasing the gas flow rate decreased the volumetric fraction of liquid in the primarily liquid portion of the pulse. It is expected that the significant change in the volumetric liquid fraction would affect the radial transport of heat and mass in a packed bed.

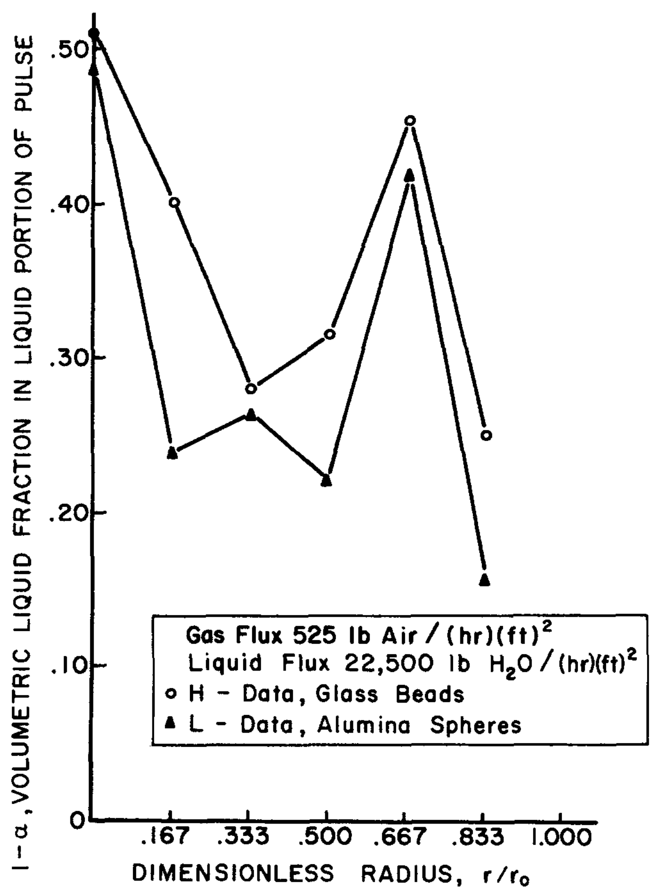

Fig. 8. Main effect due to packing.

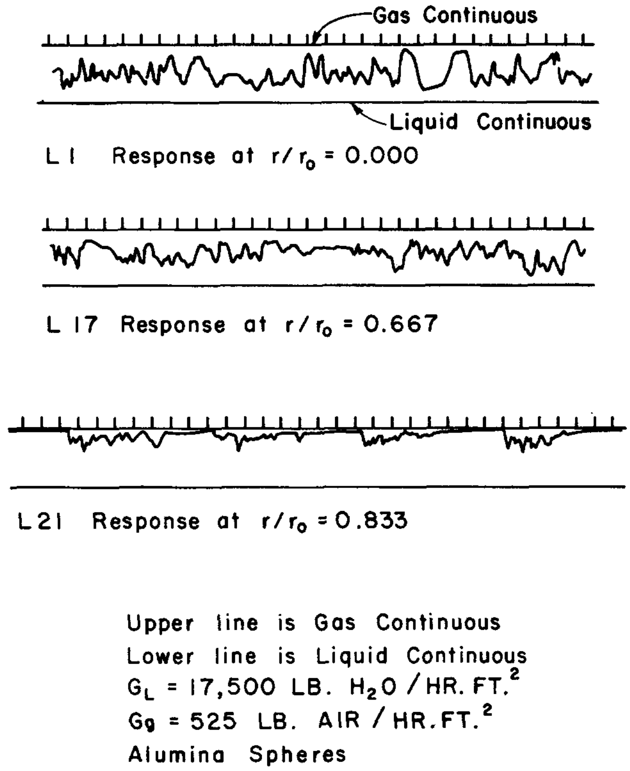

Fig. 9. Comparison of probe response at different radial positions in packed bed.

Probe Position and Model Modification

The main effect due to the radial position in the packed bed was significant. The trends as shown in Figure 8 are the same in all other data that were obtained. The striking features of Figure 8 are the high volumetric liquid fraction in the primarily liquid portion of the pulse at radial positions centered about $r/r_0 = 0.000$ and 0.667. Moving away from the center of the bed, the volumetric liquid fraction decreased to a lower value and then increased to a much higher value centered about $r/r_0 = 0.667$. Thereafter, it decreased to a minimum value centered about $r/r_0 = 0.833$. According to both Weekman (*14*) and Wulfert (*15*), at the wall ($r/r_0 = 1.0$) the volumetric liquid fraction equals 1, that is, the liquid is continuous. The large concentration of liquid in the center was not surprising, since Weekman's liquid distribution measurements indicated that large volumes of liquid flow down the center of the bed. Weekman concluded from impact tube data that the flow in the center was spray type of flow. However, Wulfert later showed that the center of the primarily liquid portion of the pulse was porous due to channels for gas flow bypass. The data obtained in this study support Wulfert's conclusion.

The apparent discontinuity in the volumetric liquid fraction at $r/r_0 = 0.667$ must be qualitatively supported and explained. In the *H* runs (noted in Table 1), four probes recorded simultaneously at angular positions 90 deg. apart. The phenomenon occurred at all four probes simultaneously. Also of importance was the fact that crisp breakoff and return to the gas continuous baseline did not occur centered about $r/r_0 = 0.000$ and 0.667, once the primarily liquid portion of the pulse had passed. Figures 9 and 10 compare the breakoff and return to the baseline at various radial positions in the bed.

TABLE 2. INTEGRATED PULSE DATA COMPARED WITH LARKINS' CORRELATION

Packing	Liquid rate, lb. water/ (hr.) (sq. ft.)	Gas rate, lb. air/ (hr.) (sq. ft.)	δ_l cm. Hg./ ft.	δ_g cm. Hg./ ft.	χ	R_l, Larkins' liquid holdup fraction	Integrated pulse value	Ratio	$\overline{(1-\alpha)}$ in liquid portion of pulse
Glass beads	17,500	525	0.68	0.43	1.26	0.188	0.142	0.758	0.476
Glass beads	17,500	750	0.68	0.73	0.965	0.165	0.120	0.725	0.398
Glass beads	22,500	525	1.05	0.43	1.56	0.211	0.132	0.625	0.437
Glass beads	22,500	750	1.05	0.73	1.22	0.187	0.123	0.656	0.410
Aluminum spheres	17,500	525	0.31	0.27	1.07	0.174	0.115	0.662	0.384
Aluminum spheres	17,500	750	0.31	0.49	0.795	0.149	0.107	0.720	0.361
Aluminum spheres	22,500	525	0.51	0.27	1.38	0.198	0.125	0.630	0.415
Aluminum spheres	22,500	750	0.51	0.49	1.02	0.171	0.102	0.600	0.341

Average ratio equals 0.672. Average $(1 - \alpha) = 0.403$.

It is a well-known fact (*1*) that for single-phase flow in a packed column, the maximum velocity occurs at approximately $r/r_0 = 0.800$. This is caused by the increase in porosity of the packing as the wall is approached from the center of the bed and before wall drag becomes important. The fluid moves with less resistance through the packing adjacent to the wall because of the increase in porosity (*11*). (In two-phase concurrent flow, the gas is considered as pushing and exerting drag on the primarily liquid portion of the pulses.)

Larkins' (*6*) liquid holdup estimations in Table 2 show that about 80% of the total free space in the packed bed is occupied by the gas. The high volumetric fraction of gas (or low liquid volumetric fraction) centered about $r/r_0 = 0.833$ might occur because this is the path of least resistance for gas flow in the operating range studied. Most of any liquid which tries to follow this same path is quickly pushed aside by the gas. The data appear to show an annular liquid "finger" extending up from the primarily liquid portion of the pulse. In addition, the liquid continuous region near the wall is frequently partially displaced from the wall.

Figure 11 illustrates the new pulsing flow model. The liquid is continuous at the wall (*14*). Centered about $r/r_0 = 0.833$ a high concentration of gas exists, and the gas travels in a channel. A finger of liquid extends from pulse to pulse at $r/r_0 = 0.000$ and an annular finger extends from pulse to pulse centered about $r/r_0 = 0.667$. The middle of the primarily liquid portion of the pulse is a porous liquid region with a high volumetric fraction of gas, indicating that the gas bypasses the liquid here also. Between the primarily liquid portion of the pulses a primarily gas continuous region exists.

Interactions

Packing/gas rate and packing/position in the bed interactions are significant. For the packing/gas rate interac-

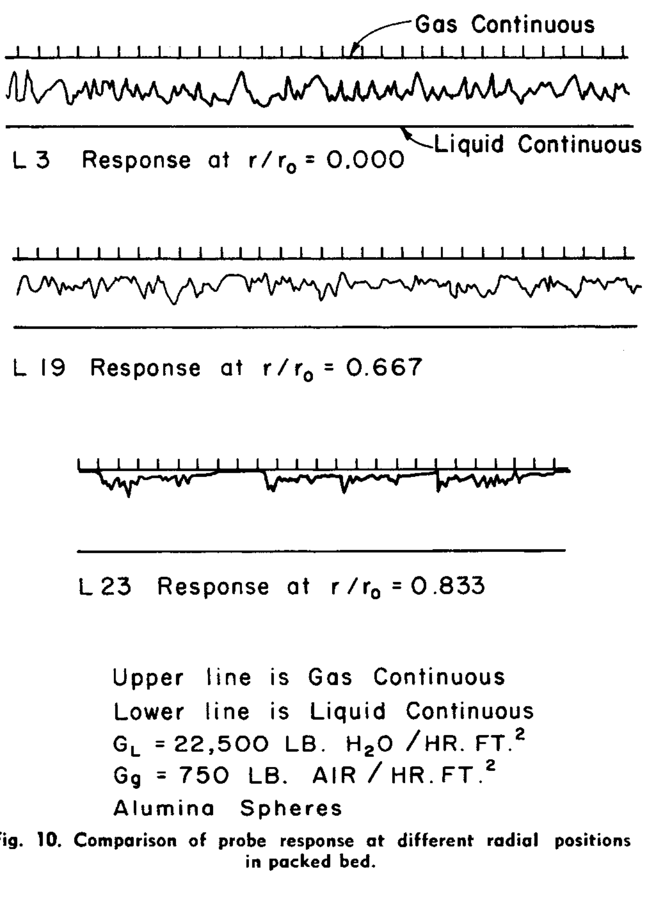

Fig. 10. Comparison of probe response at different radial positions in packed bed.

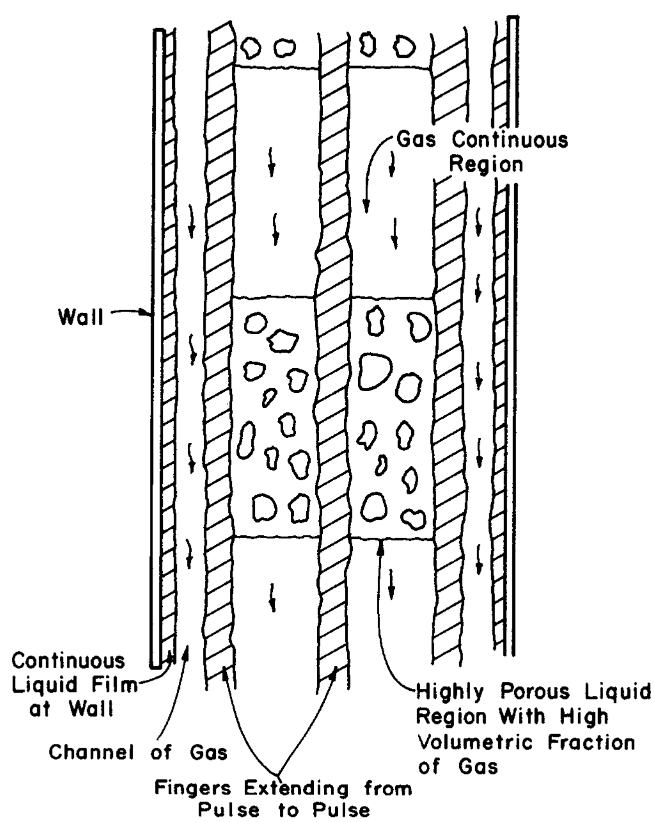

Fig. 11. Proposed pulsing flow model.

tion, the sum of squares and mean squares indicates that this is not a large interaction. However, the packing/position in the bed interaction is highly significant. Before a satisfactory explanation for this interaction can be given, further investigations with different packings is warranted.

Integrated Data from Pulses Compared to Holdup Data

The volumetric liquid fraction of the primarily liquid portion of the pulse was integrated across the radius of the packed bed to obtain liquid holdup information. Photographic work by Weekman (*14*) indicates that the height of the primarily liquid portion of the pulse is approximately 30% of the total height of the pulse for the operating range studied in this work. In Table 2 the values of the integrated experimental data are compared to values from Larkins' correlation (*6*). The integrated values are somewhat less than the correlation and on the average indicate (1) 67% of the liquid is present in 30% of the total pulse (primarily liquid portion of the pulse); (2) 33% of the liquid is present in 70% of the total pulse (primarily gas portion of the pulse). By subtraction, the primarily gas portion of the pulse contains 0.08 volumetric liquid fraction. The primarily liquid portion of the pulse contains on the average 0.40 volumetric liquid fraction (based on the free space available in the bed).

The calculated volumetric liquid fraction of 0.08 in the primarily gas portion of the pulse is the approximate expected value for the connate water in this packed bed of spheres (3). Connate water is the remaining liquid in a packed bed if the bed is filled with water, drained, and the remaining volumetric liquid fraction measured. (This 0.08 fraction represents 33% of the total liquid holdup value in the column as calculated from Larkins' correlation minus the liquid holdup obtained by integrating the primarily liquid portion of this pulse.)

CONCLUSIONS

The significant variables and interactions in order of importance are position in the bed, packing, gas rate, packing/probe position in the bed interaction, and packing/gas rate interaction.

The difference in response of the packings is due to the total liquid holdup variation which depends on the porosity of the packing (since in this case both packings were spherical). The liquid rate is not significant. In increasing only liquid flow the fluid mechanics of the pulse remains essentially the same. Increasing only the gas rates increases the volumetric gas fractions in the primarily liquid portion of the pulse.

A new phase distribution model is proposed which includes liquid fingers at the center of the pulse and centered about $r/r_0 = 0.667$. A gas channel is present centered about $r/r_0 = 0.833$, and low liquid fractions are present in the remainder of the radial positions. This gas channel would provide a zone of high resistance to radial heat and mass transfer in a packed bed.

The average volumetric liquid fraction of the primarily liquid portion of the pulse is 0.40, while the volumetric liquid fraction of the primarily gas portion of the pulse is 0.08.

It is possible that the packing/probe position in the bed interaction could indicate a dependence of the finger of liquid on the column diameter-to-particle diameter ratio.

Future work includes the study of dispersion from a point source within the bed for the pulsing flow regime and theoretical development of models for pulse flow.

ACKNOWLEDGMENT

The authors acknowledge the financial support of the Procter and Gamble Company, American Cyanamid Company, and Purdue University.

Our appreciation is expressed to V. W. Weekman, Jr., and K. J. Wulfert, Jr., for their previous work on the column system used in this work.

NOTATION

A_G = integrated area under trace in gas continuous system
A_L = integrated area under trace in liquid continuous system
A_{RG} = integrated area ratio in gas continuous system
A_{RL} = integrated area ratio in liquid continuous system
G_g = superficial gas flux, lb./(hr.)(sq.ft.)
G_l = superficial liquid flux, lb./(hr.)(sq.ft.)
h = difference in liquid and gas continuous baselines
l = width of probe response
n = exponent in calibration equation
P = probability
r/r_0 = dimensionless radius
R_l = liquid holdup in packed column, volumetric fraction
V_{SG} = superficial gas velocity in calibration tube, ft./sec.
V_∞ = terminal velocity of bubble, ft./sec.

Greek Letters

α = volumetric gas fraction in packed bed
α_T = volumetric gas fraction in calibration system
$(1-\alpha)$ = volumetric liquid fraction in packed bed
$\overline{(1-\alpha)}$ = average volumetric liquid fraction in liquid portion of the pulse
δ_g = pressure drop of gas flowing alone in the packed bed, cm. Hg/ft.
δ_l = pressure drop of liquid flowing alone in the packed bed, cm. Hg/ft.
χ = two-phase flow coefficient
ϵ = void of packing

LITERATURE CITED

1. Cairns, E. J., and J. M. Prausnitz, *Ind. Eng. Chem.*, **51**, 1441 (1959).
2. Dodds, W. S., L. F. Stutzman, B. J. Sollami, and R. J. McCarter, *AIChE J.*, **6**, 390 (1960).
3. Hochmann, J. M., and E. Effron, *Ind. Eng. Chem. Fundamentals*, **8**, 63 (1969).
4. Hoftyzer, P. J., *Trans. Inst. Chem. Eng.*, **42**, T109 (1964).
5. Lapidus, Leon, *Ind. Eng. Chem. Fundamentals*, **49**, 1000 (1957).
6. Larkins, R. P., R. R. White, and D. W. Jeffrey, *AIChE J.*, **7**, 231 (1961).
7. Nicklin, D. J., *Chem. Eng. Sci.*, **17**, 693 (1962).
8. Prost, C., *ibid.*, **22**, 1283 (1967).
9. Reiss, L. P., *Ind. Eng. Chem. Proc. Design Devel.*, **6**, 486 (1967).
10. Rhodes, E., and D. S. Scott, "Cocurrent Gas Liquid Flow," p. 81, Plenum Press, New York (1969).
11. Roblee, L. H., R. M. Baird, and J. W. Tierney, *AIChE J.*, **4**, 460 (1958).
12. Turpin, J. L., and R. L. Huntington, *ibid.*, **13**, 1196 (1967).
13. Weekman, V. W., and J. E. Myers, *ibid.*, **10**, 951 (1964).
14. Weekman, V. W., Ph. D. thesis, Purdue Univ., Lafayette, Ind. (1963).
15. Wulfert, K. J., M.S. thesis, Purdue Univ., Lafayette, Ind. (1969).

Manuscript received June 24, 1970; paper accepted November 5, 1970.